

Edinburgh 2006/05
 PSI-06-04
 ZU-TH 05/06
 January 2006

Towards LHC phenomenology at the loop level: A new method for one-loop amplitudes

T. Binoth^{a*}, M. Ciccolini^b and G. Heinrich^{c†}

^aSchool of Physics, University of Edinburgh, EH9 3JZ Edinburgh, UK

^bPaul Scherrer Institut, Würenlingen und Villigen, CH-5232 Villigen PSI, Switzerland

^cInstitute for Theoretical Physics, University of Zürich, CH-8057 Zürich, Switzerland

A precise understanding of LHC phenomenology requires the inclusion of one-loop corrections for multi-particle final states. In this talk we describe a semi-numerical method to compute one-loop amplitudes with many external particles and present first applications.

1. Introduction

In this decade high energy physics will explore the TeV scale with hadron colliders like the Tevatron and the LHC. The Tevatron experiments already have provided rich information on electroweak, jet and heavy quark physics. These data and their theoretical description are of major importance for Higgs and New Physics searches. A detailed understanding of Standard Model processes is indispensable to discriminate between signals and backgrounds in this respect. This is especially true in hadronic collisions at the TeV scale because of the complicated multi-particle final states. It is well known that leading order QCD predictions are generally plagued by large renormalization/factorization scale uncertainties. Only the inclusion of higher order corrections may lead to more stable predictions, as leading logarithmic contributions typically cancel in that case. Moreover, it should be emphasized that not only the overall normalization is an issue here, higher order corrections can also change the *shapes* of distributions. The knowledge of distribution shapes is particularly important in those cases where backgrounds measured

in a low signal region have to be extrapolated to signal regions by using theoretical predictions. A prominent example is the Higgs discovery mode $H \rightarrow WW \rightarrow l\bar{\nu} l'\nu'$.

The computation of one-loop corrections to multi-particle final states is a complex task, as the combinatorial growth of expressions together with complicated denominator structures hinders a straightforward evaluation of the amplitudes. Due to its phenomenological relevance, a lot of activity has been going on in this direction during the last years [1,2,3,4,5,6,7,8,9,10,11,12].

In this talk, a method [5] for the evaluation of one-loop diagrams occurring in multi-particle computations at NLO is presented. This approach allows for a good analytical control over the expressions, but also provides stable numerical representations in phase space regions which typically pose numerical problems. Some applications are also presented.

2. Reduction formalism

Any given amplitude can be represented as a linear combination of Feynman diagrams, which correspond to linear combinations of tensor integrals. We define tensor integrals by

$$I_N^{n,\mu_1\ldots\mu_r}(a_1,\ldots,a_r) = \int d\bar{k} \frac{q_{a_1}^{\mu_1} \cdots q_{a_r}^{\mu_r}}{(q_1^2 - m_1^2 + i\delta) \cdots (q_N^2 - m_N^2 + i\delta)}, \quad (1)$$

*Work supported by Deutsche Forschungsgemeinschaft (DFG), grant number Bi1050/1-2.

†Work supported by the Swiss National Science Foundation (SNF), contract number 200020-109162.

where $q_i = k + r_i$, $r_j - r_{j-1} = p_j$, $\sum_{j=1}^N p_j = 0$ and $d\bar{k} = d^n k / (i\pi)^{n/2}$. One of the advantages of this representation is that the combinations $q_i = k + r_i$ appear naturally (e.g. fermion propagators). When introducing form factors, the Lorentz structure is carried by difference vectors $\Delta_{ij}^\mu = r_i^\mu - r_j^\mu$ and $g^{\mu\nu}$. As an example, consider the rank 2 case

$$I_N^{n, \mu_1 \mu_2}(a_1, a_2; S) = \sum_{l_1, l_2 \in S} \Delta_{l_1 a_1}^{\mu_1} \Delta_{l_2 a_2}^{\mu_2} A_{l_1 l_2}^{N, 2}(S) + g^{\mu_1 \mu_2} B^{N, 2}(S).$$

The kinematical information is encoded in the matrix $\mathcal{S}_{ij} = (r_i - r_j)^2 - m_i^2 - m_j^2$ which is the characteristic object in any Feynman parameter integral. After momentum integration, the scalar N -point function is of the form

$$I_N^n(S) = (-1)^N \Gamma(N - \frac{n}{2}) \times \int \prod_{i=1}^N dz_i \delta(1 - \sum_{l=1}^N z_l) (R^2)^{\frac{n}{2} - N} R^2 = -\frac{1}{2} \sum_{i,j=1}^N z_i \mathcal{S}_{ij} z_j - i\delta.$$

Tensor integrals lead to additional factors z_i in the numerator. As a shorthand notation we use the ordered set S of propagator labels instead of the matrix \mathcal{S} as our function arguments. A matrix corresponding to an integral with propagator $1/P_j = 1/(q_j^2 - m_j^2 + i\delta)$ omitted (“pinched”) corresponds to an index set $S \setminus \{j\}$. The reduction of scalar integrals can now be written as

$$I_N^n(S) = \sum_{i \in S} b_i(S) \int d\bar{k} \frac{P_i}{\prod_{j \in S} P_j} + \int d\bar{k} \frac{1 - \sum_{i \in S} b_i(S) P_i}{\prod_{j \in S} P_j} \stackrel{!}{=} I_{div}(S) + I_{fin}(S).$$

One can show [5] that if $\sum_{i \in S} b_i(S) \mathcal{S}_{ij} = 1$ is fulfilled, then

$$I_{fin}(S) = -B(S)(N - n - 1) I_N^{n+2}(S), \\ B(S) = \sum_{i \in S} b_i(S), \\ B(S) \det \mathcal{S} = (-1)^{N+1} \det G, \quad G_{ij} = 2r_i \cdot r_j,$$

where the subscript “*fin*” indicates that the respective integral is infrared finite. The algorithm allows to isolate recursively all infrared poles in terms of three-point integrals.

The reduction of tensor integrals is performed in a similar way. We add and subtract a linear combination of pinched terms and adjust the coefficients conveniently:

$$I_N^{n, \mu_1 \dots \mu_r}(a_1, \dots, a_r; S) = - \sum_{j \in S} \mathcal{C}_{j a_1}^{\mu_1} \int d\bar{k} \frac{P_j q_{a_2}^{\mu_2} \dots q_{a_r}^{\mu_r}}{\prod_{i \in S} P_i} + \int d\bar{k} \frac{[q_{a_1}^{\mu_1} + \sum_{j \in S} \mathcal{C}_{j a_1}^{\mu_1} P_j] q_{a_2}^{\mu_2} \dots q_{a_r}^{\mu_r}}{\prod_{i \in S} P_i} \stackrel{!}{=} I_{div} + I_{fin}$$

If $\sum_{i \in S} \mathcal{C}_{i a}^\mu(S) \mathcal{S}_{ij} = \Delta_{j a}^\mu$ for all $j \in S$, then I_{fin} is proportional to a sum of higher dimensional integrals I_N^{n+2m} ($m > 0$) and thus IR finite. In this way, the tensor integrals also can be reduced to a set of (potentially IR divergent) integrals with lower rank and less propagators and an infrared finite part. If \mathcal{S} is invertible, i.e. for $N < 7$ and non-exceptional kinematics, one finds

$$\mathcal{C}_{i a}^\mu(S) = \sum_{j \in S} (\mathcal{S}^{-1})_{ij} \Delta_{j a}^\mu,$$

otherwise the pseudo-inverse H_{ij} of the Gram matrix G can be used [5,12] to obtain

$$\mathcal{C}_{i b}^\mu = - \sum_{j \in S \setminus \{a\}} H_{ij} \Delta_{j a}^\mu + W_i^\mu, \quad i \in S \setminus \{a\} \\ \mathcal{C}_{a b}^\mu = - \sum_{j \in S \setminus \{a\}} \mathcal{C}_{j b}^\mu,$$

where the vectors W_i^μ span the kernel of G .

If $N > 5$, one finds that all higher dimensional integrals drop out as a consequence of $\text{rank}(\mathcal{S}) = \min(N, 6)$. Therefore one has for $N > 5$:

$$I_N^{n, \mu_1 \dots \mu_r}(a_1, \dots, a_r; S) = - \sum_{j \in S} \mathcal{C}_{j a_r}^{\mu_r} I_{N-1}^{n, \mu_1 \dots \mu_{r-1}}(a_1, \dots, a_{r-1}; S \setminus \{j\}).$$

Note that N and the tensor rank are reduced at the same time. The case $N = 5$ is

more involved, but a reduction scheme has been worked out where no higher dimensional integrals I_N^{n+2m} ($m > 0$) are present for $N > 4$ and no inverse Gram determinants are introduced [5]. As in the scalar case, an algebraic separation of IR poles, contained in 3-point integrals only, is achieved iteratively.

Application of the reduction formulas to integrals of rank $r \leq 2$ leads, for any N , to form factors in terms of simple scalar integrals. For rank $r > 2$, reduction to purely scalar integrals with $N = 3, 4$ is no longer possible without introducing a tower of higher dimensional integrals. To avoid the latter, we use integrals with Feynman parameters in the numerator as reduction endpoints. Explicit representations for all form factors for $r \leq N \leq 5$ can be found in [5]. The form factors are expressed in terms of the following basis integrals

$$\begin{aligned}
I_3^n(j_1, \dots, j_r) &= -\Gamma\left(3 - \frac{n}{2}\right) \\
&\times \int_0^1 \prod_{i=1}^3 dz_i \frac{z_{j_1} \dots z_{j_r} \delta(1 - \sum_{l=1}^3 z_l)}{(-\frac{1}{2} z \cdot \mathcal{S} \cdot z)^{3-n/2}}, \quad (2) \\
I_3^{n+2}(j_1) &= -\Gamma\left(2 - \frac{n}{2}\right) \\
&\times \int_0^1 \prod_{i=1}^3 dz_i \frac{z_{j_1} \delta(1 - \sum_{l=1}^3 z_l)}{(-\frac{1}{2} z \cdot \mathcal{S} \cdot z)^{2-n/2}}, \\
I_4^{n+2}(j_1, \dots, j_r) &= \Gamma\left(3 - \frac{n}{2}\right) \\
&\times \int_0^1 \prod_{i=1}^4 dz_i \frac{z_{j_1} \dots z_{j_r} \delta(1 - \sum_{l=1}^4 z_l)}{(-\frac{1}{2} z \cdot \mathcal{S} \cdot z)^{3-n/2}}, \quad (3) \\
I_4^{n+4}(j_1) &= \Gamma\left(2 - \frac{n}{2}\right) \\
&\times \int_0^1 \prod_{i=1}^4 dz_i \frac{z_{j_1} \delta(1 - \sum_{l=1}^4 z_l)}{(-\frac{1}{2} z \cdot \mathcal{S} \cdot z)^{2-n/2}},
\end{aligned}$$

where $r_{\max} = 3$ in eqs. (2) and (3), and of course purely scalar integrals $I_3^n, I_3^{n+2}, I_4^{n+2}, I_4^{n+4}$ are also basis integrals. We provide two alternatives for the evaluation of the basis integrals. On one hand, an algebraic reduction to scalar integrals can be performed. This leads to representations with inverse Gram determinants. As long as the Gram determinant – or more precisely the related quantity $B \sim \det G / \det \mathcal{S}$ – is sufficiently large,

such a representation is numerically safe. On the other hand, if the Gram determinants become smaller than a certain cut parameter Λ , a direct numerical evaluation of the building blocks of the reduction is performed.

3. Numerical evaluation of basis integrals

We show now how a numerically stable evaluation of the integrals

$$\begin{aligned}
I_N^d(j_1, \dots, j_r) &= (-1)^N \Gamma(N - \frac{d}{2}) \\
&\int_0^\infty d^N x \delta(1 - \sum_{l=1}^N x_l) \frac{x_{j_1} \dots x_{j_r}}{(x \cdot \mathcal{S} \cdot x/2 + i\delta)^{N-d/2}}
\end{aligned}$$

for the required cases $N \leq 4$, $r \leq 3$, $d = 4 - 2\epsilon, 6, 8 - 2\epsilon$ can be achieved. Let us focus on the basis integrals with $d = 4 - 2\epsilon$, $N = 3$ and $d = 6$, $N = 4$. The other cases contain UV divergencies which are isolated in terms of external $\Gamma(N - d/2)$ factors. After expansion of the integrand in ϵ , the pole part is a trivial integral and the finite part is a logarithmic integral which can be treated with the same contour deformation methods as discussed below. IR divergencies are only present for $N = 3$ and $d = 4 - 2\epsilon$. For the IR divergent integrals explicit analytical formulas can be found in [5]. The numerical evaluation of the remaining IR finite integrals is problematic due to kinematical singularities, which occur if the quadratic form $x \cdot \mathcal{S} \cdot x$ changes sign. We propose the following solution: We first make a sector decomposition

$$1 = \sum_{l=1}^N \theta(x_l > x_1, \dots, x_{l-1}, x_{l+1}, \dots, x_N).$$

The integral is thus split into N terms:

$$\begin{aligned}
I_N^d(j_1, \dots, j_r) &= (-1)^N \Gamma(N - d/2) \\
&\sum_{l=1}^N J_l(N, d, j_1, \dots, j_r).
\end{aligned}$$

In sector l one applies the variable transformation $x_j = t_j x_l$ for $(j < l)$, $x_j = t_{j-1} x_l$ for $(j > l)$ and integrates out x_l with the δ distribution. Defining

$\vec{T} = (t_1, \dots, t_{l-1}, 1, t_l, \dots, t_{N-1})$ gives

$$J_l(N, d, j_1, \dots, j_r) = \int_0^1 d^{N-1}t \left(\sum_{j=1}^N T_j \right)^{N-d-r} \times \frac{T_{j_1} \dots T_{j_r}}{\left(T \cdot \mathcal{S} \cdot T/2 - i\delta \right)^{N-d/2}}.$$

$Q(t) = T \cdot \mathcal{S} \cdot T/2$ leads to singular behaviour if

$$Q(t) = \frac{1}{2} \sum_{j,k=1}^{N-1} A_{jk} t_j t_k + \sum_{j=1}^{N-1} B_j t_j + C = 0$$

A, B, C are defined by \mathcal{S} . For the sector integrals J_l the following contour deformation, parametrized by $\alpha, \beta > 0, \lambda \geq 0$, leads to smooth integrands [5,14]

$$\vec{x}(\vec{t}) = \vec{t} - i \vec{\tau}(\vec{t})$$

$$\tau_k = \lambda t_k^\alpha (1 - t_k)^\beta \sum_{j=1}^{N-1} (A_{jk} t_j + B_k)$$

While $\lambda \nabla \cdot Q$ controls the size of the deformation, the parameters α, β control the smoothness of the deformation at the integration boundaries. There are situations where the contour deformation is not possible. This happens if $\nabla \cdot Q = 0$ and $Q = 0$. This exceptional kinematic situation occurs in the presence of normal or anomalous thresholds and cannot be avoided. The way to deal with it is to split the integrations at $t_j = -\sum_{l=1}^{N-1} A_{jl}^{-1} B_l$ if necessary. Typically the proposed contour deformation method works well, although the CPU time for evaluating a basis integral is much larger than evaluating the corresponding analytical representations. The conclusion for the practitioner is to use the fast and accurate algebraic formulas for the “bulk” of the phase space and switch to the slow but reliable numerical evaluation near critical phase space regions. In the case of 4-point functions this looks schematically as shown in Fig. 1.

4. Applications

Our reduction algorithm has been applied so far to several processes [15,16,17,18]. Here we focus on two of them. First, off-shell vector boson pair production via gluon fusion at the LHC,

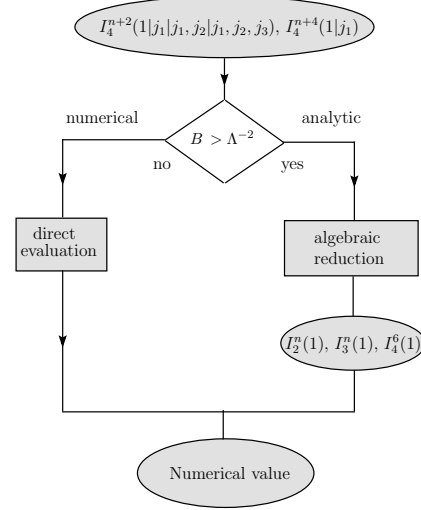


Figure 1. Schematical evaluation of basic box functions. Λ is a user-defined parameter serving as a switch between analytic/numerical representations.

which is a background for the $gg \rightarrow H \rightarrow W^* W^*$ channel [18]. Although only box graphs occur, the large number of invariants $(s, t, p_3^2, p_4^2, m_b, m_t)$ makes the process sufficiently involved to provide a good testing ground for our method. The helicity amplitudes Γ^{++}, Γ^{+-} were computed in a modular way. The amplitude was decomposed into gauge invariant terms and was reduced completely to $d = 6$ box, $d = 4$ triangle and bubble integrals. As an illustration we show the invariant mass distribution of the charged lepton pair for $gg \rightarrow W^* W^* \rightarrow l\bar{\nu} l'\nu'$ in Fig. 2. Numerically instable regions are confined to very small phase space regions which do not contribute to the result inside the errors.

Another application of our reduction procedure was the first direct computation of the $gg \rightarrow \gamma\gamma g$ one-loop amplitude. Although the amplitude could be indirectly deduced from the $gg \rightarrow ggg$ loop result [13], it was shown that very compact results could be obtained for all six independent helicity amplitudes [17]. This result is

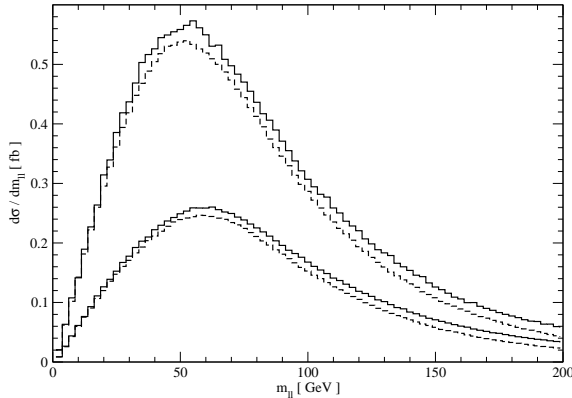


Figure 2. Invariant mass distribution of the charged lepton pair for $gg \rightarrow W^*W^* \rightarrow l\bar{\nu}l'\nu'$. The two sets of curves are the LHC prediction with (lower) and without (upper) standard cuts. The effect of the third generation massive quark loop leads to a slight enhancement (full) compared to the case with two massless generations (dashed). For parameter choices see [18].

of relevance for the Higgs boson search channel $PP \rightarrow H + \text{jet} \rightarrow \gamma\gamma \text{ jet}$ at the LHC.

5. Summary

For a precise understanding of LHC phenomenology, NLO precision for multi-particle amplitudes is mandatory. We have presented a new semi-numerical approach for 1-loop multi-leg processes which is valid for an arbitrary number of massless as well as massive internal/external particles. It allows to isolate IR divergences transparently and in an automated way from the amplitude. Our reduction algorithm uses a set of building blocks which can be evaluated either analytically, if the inherent Gram determinants are sufficiently large, or numerically, avoiding inverse Gram determinants and the associated instabilities completely. To achieve the latter, a multi-dimensional contour deformation method for 1-loop parameter integrals was developed. The full potential of the contour deformation method for

one- and multi-loop Feynman diagrams is being further investigated.

We have shown that our analytical reduction method works well for processes of phenomenological interest like photon pair plus jet production or off-shell vector boson pair production at the LHC. Applications to LHC processes with a larger number of external particles are presently being studied.

REFERENCES

1. A. Denner and S. Dittmaier, Nucl. Phys. B **734** (2006) 62.
2. A. Denner, S. Dittmaier, M. Roth and L. H. Wieders, arXiv:hep-ph/0505042.
3. C. Anastasiou and A. Daleo, arXiv:hep-ph/0511176.
4. R. K. Ellis, W. T. Giele and G. Zanderighi, arXiv:hep-ph/0508308.
5. T. Binoth, J. P. Guillet, G. Heinrich, E. Pilon and C. Schubert, JHEP **0510** (2005) 015.
6. A. van Hameren, J. Vollinga and S. Weinzierl, Eur. Phys. J. C **41** (2005) 361.
7. W. T. Giele and E. W. N. Glover, JHEP **0404** (2004) 029.
8. Z. Nagy, D. E. Soper, JHEP **0309** (2003) 055.
9. T. Binoth, G. Heinrich and N. Kauer, Nucl. Phys. B **654** (2003) 277.
10. G. Duplancic and B. Nizic, Eur. Phys. J. C **35** (2004) 105.
11. A. Ferroglia, M. Passera, G. Passarino and S. Uccirati, Nucl. Phys. B **650** (2003) 162.
12. T. Binoth, J. P. Guillet and G. Heinrich, Nucl. Phys. B **572** (2000) 361.
13. Z. Bern, L. J. Dixon and D. A. Kosower, Phys. Rev. Lett. **70** (1993) 2677.
14. Y. Kurihara and T. Kaneko, hep-ph/0503003.
15. T. Binoth, J. P. Guillet, G. Heinrich and C. Schubert, Nucl. Phys. B **615** (2001) 385.
16. T. Binoth, Nucl. Phys. Proc. Suppl. **116** (2003) 387.
17. T. Binoth, J. P. Guillet and F. Mahmoudi, JHEP **0402** (2004) 057.
18. T. Binoth, M. Ciccolini, N. Kauer and M. Krämer, JHEP **0503** (2005) 065. Article discussing massive case in preparation.